



## Cracking of Two-phase Ceramics under Uniaxial Compression Deformation

Tomasz SADOWSKI<sup>1)</sup>, Liviu MARSAVINA<sup>2)</sup>, Eduard M. CRACIUN<sup>3)</sup>

<sup>1)</sup> *Lublin University of Technology*  
*Department of Solid Mechanics*  
Nadbystrzycka 40, 20-618 Lublin, Poland  
e-mail: t.sadowski@pollub.pl

<sup>2)</sup> *Polytechnica University Timisoara*  
*Department Strength of Materials*  
Blvd. M. Viteazu, No 1, Timisoara 300222, Romania

<sup>3)</sup> *“Ovidius” University of Constanta*  
*Faculty of Mechanical, Industrial and Maritime Engineering*  
Bd. Mamaia 124, 900527, Constanta, Romania

Two-phase ceramics have a non-linear and complex overall response to applied loads due to composition of two different phases with initial porosity, development of limited plasticity and internal microdefects. These microdefects cause stress concentrations and locally change the state of stress, which results in the development of mesocracks leading to macrocracks. In this article, a multiscale approach was applied to the modelling of the two-phase ceramics response under compression deformation. This allowed to include different phenomena at micro-, meso- and macro-scales.

**Key words:** two-phase ceramic materials, cracking under compression, multiscale modelling.

### 1. INTRODUCTION

The currently used innovative materials are different types of composites consisting of various phases, which are subjected to complicated manufacturing process to get the required properties for specific engineering applications, e.g., [1, 2]. The engineering of materials allows for designing of almost arbitrary internal structure of the composites specifically for industrial demands. Functionally graded materials possessing gradation of the material properties are good example of modern composites, e.g., [3]. Advanced ceramic composites can be built up as a sequence of layers, e.g., as TBC covering of turbine blades (e.g., [4, 5]).

2-phase ceramics composite, like  $\text{Al}_2\text{O}_3/\text{ZrO}_2$ , is frequently used as a thermal barrier protection for different structures, e.g., [4, 5]. In this paper, we focus on modelling of crack propagation in this material under compressive deformation, extending the research conducted in [6, 7]. The matrix material is  $\text{Al}_2\text{O}_3$ , whereas the second phase  $\text{ZrO}_2$  has different thermal expansion coefficient, which causes an initiation of small amount of microcracks and micropores during the cooling process. These microdefects cause stress concentrations, which result in the development of mesocracks leading to macrocracks. The paper proposes mesoscale model, applying averaging procedure over the representative surface element (RSE), for description of different cracking phenomena at micro- and meso-scales, which develop during the compression.

## 2. FORMULATION OF THE CONSTITUTIVE EQUATIONS FOR 2-PHASE CERAMICS

Degradation scenario of the considered  $\text{Al}_2\text{O}_3/\text{ZrO}_2$  can be described as follows:

- microcracks and micropores are initiated inside the grains or grain boundaries by mismatch of the thermal expansion coefficient of 2 phases during the technological cooling. The microcracks nucleated inside the grains move to grain boundaries, at which they can be arrested or can spread along the nearest grain boundary. This results from a significantly less fracture toughness of grain boundaries,
- at mesoscopic level, we observe set of grains, i.e., the RSE. Mesocracks are the basic elements of the defect structure inside polycrystal in early stage of deformation. Their diameters correspond to the single straight facet of the structure of grain boundaries. In an advanced stage, kinked and wing (zig-zag) cracks appear in the RSE due to the development of deformation process in the ceramic composite, Fig. 1a.

Taking into account the above information a constitutive equation should be:

$$(2.1) \quad \bar{\varepsilon}_i = \bar{S}_{ik}^e(\sigma_m, p_f, p_o, N_c^{(s)})\sigma_k,$$

where  $\bar{\varepsilon}_i$  is the strain vector,  $\bar{S}_{ik}^e$  is the elastic compliance matrix,  $\sigma_k$  is the stress vector,  $p_f$  is the volume content of the second phase ( $\text{ZrO}_2$ ),  $p_o$  is the porosity parameter, and  $N_c^{(s)}$  are sets of parameters defining the presence of different kinds of defects “s” developing inside the material, Fig. 1a. Figure 1b presents the fracture surface of the analyzed ceramics after failure in compression.

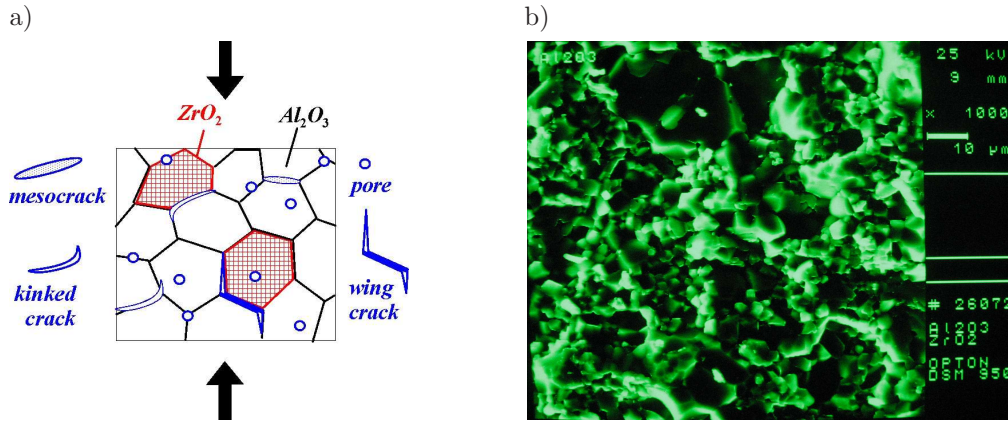


FIG. 1. a) internal structure of the CMC in advanced stage of deformation, b) fracture surface.

In order to describe porosity presence in the ceramic composite we applied the material model proposed in [8].

The wing cracks have the most important influence on the mechanical response of the RSE, Fig. 2a. They are created from mesocracks of the length  $2c^{(s)}$  by kinking and growing along the grain boundaries. This is due to the fact that the fracture surface energy of the grain boundary  $\gamma_{gb}$  in the polycrystalline com-

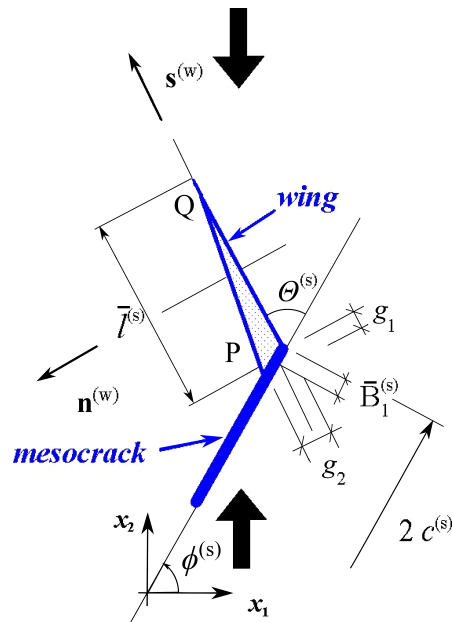


FIG. 2. Geometric characteristics of the wing crack tip.

posite is significantly smaller in comparison to the fracture surface energy of the grain  $\gamma_g$ . The set of the wing cracks create the following additional strains [9]:

$$(2.2) \quad \varepsilon_i^{\text{cr(wc)}} = \frac{\pi N_c^{(\text{wc})}}{E_0^{\text{comp}}} \left[ \begin{aligned} & \frac{2}{A} \int_{D_m}^{D_M} \left[ \int_{\phi_1^{(\text{wc})}}^{\phi_2^{(\text{wc})}} \overline{M}_{ij}^{(\text{mc})}(\phi) \sigma_j(\phi) p_3(\phi) \left( \frac{D}{4} \right)^2 p_2(D) d\phi \right] dD \\ & + \int_{\bar{l}_1}^{\bar{l}_2} p_{k_1}(\bar{l}) \left[ \int_{\theta_1 + \phi_1^{(\text{wc})}}^{\theta_2 + \phi_2^{(\text{wc})}} M_{ij}^{(\text{wc})}(\phi, \theta) \sigma_j(\phi) p_{k_2}(\theta + \phi) d(\theta + \phi) \right] \bar{l} d\bar{l} \\ & + \frac{c^2}{A} \int_{\bar{l}_1}^{\bar{l}_2} p_{k_1}(\bar{l}) \left[ \int_{\theta_1 + \phi_1^{(\text{wc})}}^{\theta_2 + \phi_2^{(\text{wc})}} M_{ij}^{(\text{wc})}(\phi, \theta) \sigma_j(\phi) p_{k_2}(\theta + \phi) d(\theta + \phi) \right] \bar{l}^2 d\bar{l} \end{aligned} \right].$$

In Eq. (2.2),  $N_c^{(\text{wc})}$  denotes the number of the wing cracks inside the RSE,  $E_0^{\text{comp}}$  – is the Young's modulus of the composite before loading process,  $\phi_1^{(\text{wc})} \leq \phi^{(\text{s})} \leq \phi_2^{(\text{wc})}$  is the fan of all mesocracks creating wings,  $p_3(\phi)$  is the distribution function of the active mesocracks,  $D$  is the length of the straight grain boundary segment,  $D_m \leq D \leq D_M$  – denotes the variation of the grain boundary length within the RSE (minimum dimension –  $D_m$ , maximum value  $D_M$ ),  $p_2(D)$  is the distribution function of  $D$ ,  $\overline{M}_{ij}^{(\text{mc})}(\phi)$  is the matrix describing the inclination angle of the active mesocracks,  $\bar{l}^{(\text{s})} = l^{(\text{s})}/c^{(\text{s})}$  is the nondimensional wing length,  $\bar{l}_1 \leq \bar{l}^{(\text{s})} \leq \bar{l}_2$  is the fan of the wing lengths inside the RSE,  $\theta_1 + \phi_1^{(\text{wc})} \leq \theta^{(\text{s})} + \phi^{(\text{s})} \leq \theta_2 + \phi_2^{(\text{wc})}$  is the fan of inclination angles of the wings,  $M_{ij}^{(\text{wc})}(\phi, \theta)$  is the matrix describing space placement of a single wing, and  $p_{k_1}(\bar{l})$  and  $p_{k_2}(\theta + \phi)$  are the distribution functions of the wing lengths and the inclination angles. The wing crack propagates when the strain energy release rate satisfies:

$$(2.3) \quad G(\sigma_r, c^{(\text{s})}, \phi^{(\text{s})}, \bar{l}^{(\text{s})}, \theta^{(\text{s})}) = \frac{1 - [\nu^{\text{comp}}(p_o)]^2}{E^{\text{comp}}(p_o)} (K_I^2 + K_{II}^2) \geq 2\gamma_{\text{gb}}.$$

The grain boundary fracture resistance  $\gamma_{\text{gb}}$  is calculated using the rule of mixture (RoM),  $\nu^{\text{comp}}(p_o)$  and  $E^{\text{comp}}(p_o)$  are initial elastic properties of the porous composite assessed by the RoM and  $K_I$  and  $K_{II}$  are stress intensity factors in tips of the mesocracks or the wing cracks (point Q, Fig. 2).

## 3. ANALYSIS OF NUMERICAL RESULTS AND CONCLUSIONS

Numerical example was calculated for the following properties of two-phase component of the analyzed composite:

- $\text{Al}_2\text{O}_3$  – the Young's modulus is equal to 400 GPa and the Poisson's ratio is equal to 0.22,  $K_{Ic} = 4.5 \text{ MPa}\cdot\text{m}^{1/2}$ ,
- $\text{ZrO}_2$  – the Young's modulus is equal to 200 GPa and the Poisson's ratio is equal to 0.25,  $K_{Ic} = 10 \text{ MPa}\cdot\text{m}^{1/2}$ .

The compression deformation process for the composite with different values of the volume content of the second phase ( $\text{ZrO}_2$ )  $p_f$  is shown in Fig. 3. The characteristic points corresponding to mesocracks and wing crack initiations are presented in Fig. 3. The increase of the volume content of the second phase  $p_f$  leads to a substantial decrease of the composite load capacity.

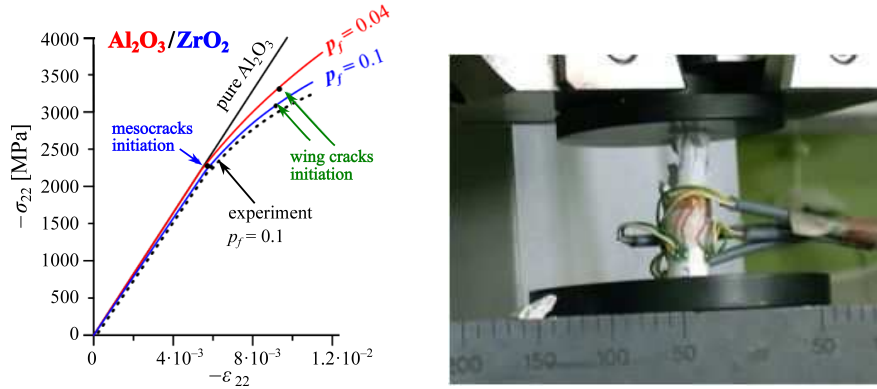


FIG. 3. Stress-strain relations for compression of the analyzed 2-phase ceramics.

Comparison of the numerical model and the experimental results for  $p_f = 0.1$  confirms accuracy of the model assumptions.

## 4. CONCLUSIONS

The obtained results lead to the following conclusions:

- volume contents of both phases constituting the analyzed composite and initial porosity strongly influenced the material behavior under mechanical loading,
- pores existing in the polycrystalline composite act as the sources of microcracks' initiations due to stress concentration under compression at their edges,
- microcracks develop under mixed mode of fracture along the straight segment of grain boundaries to form mesocracks,

- the dominant mode of mesocracks propagation is intergranular by kinking to create the wing cracks,
- the wing cracks develop in unstable manner, when criterion (2.3) is satisfied, both fracture modes: intergranular and transgranular are possible, Fig. 1b.

#### ACKNOWLEDGMENT

This work was financially supported by the Ministry of Science and Higher Education (Poland) within the statutory research number S/20/2016 (Lublin University of Technology).

#### REFERENCES

1. GÖMZE L.A., GÖMZE L.N., *Alumina-based hetero-modulus ceramic composites with extreme dynamic strength – phase transformation of  $Si_3N_4$  during high speed collision with metallic bodies*, *Építőanyag – Journal of Silicate Based and Composite Materials*, **61**(2): 38–42, 2009, doi: 10.14382/epitoanyag-jsbcm.2009.7.
2. GÖMZE L.A., GÖMZE L.N., *Ceramic based lightweight composites with extreme dynamic strength*, *IOP Conference Series: Materials Science and Engineering*, **47**(1): 012033–012038, 2013, doi: 10.1088/1757-899X/47/1/012033.
3. BIRMAN V., BRYD L.W., *Modelling and analysis of functionally graded materials and structures*, *ASME, Applied Mechanics Review*, **60**(5): 195–216, 2007, doi: 10.1115/1.2777164.
4. SADOWSKI T., GOLEWSKI P., *The influence of quantity and distribution of cooling channels of turbine elements on level of stresses in the protective layer TBC and the efficiency of cooling*, *Computational Materials Science*, **52**(1): 293–297, 2012, doi: 10.1016/j.commatsci.2011.02.027.
5. SADOWSKI T., GOLEWSKI P., *Detection and numerical analysis of the most efforted places in turbine blades under real working conditions*, *Computational Materials Science* **64**: 285–288, 2012, doi: 10.1016/j.commatsci.2012.02.048.
6. SADOWSKI T., MARSAVINA L., *Multiscale modelling of two-phase Ceramic Matrix Composites*, *Computational Materials Science*, **50**(4): 1336–1346, 2011, doi: 10.1016/j.commatsci.2010.04.011.
7. SADOWSKI T., PANKOWSKI B., *Numerical modelling of two-phase ceramic composite response under uniaxial loading*, *Composite Structures*, **143**: 388–394, 2016, doi: 10.1016/j.compstruct.2016.02.022.
8. KACHANOV M., *On effective moduli of solids with cavities and cracks*, *International Journal of Fracture*, **59**(1): R17–R21, 1993, doi: 10.1007/BF00032223.
9. SADOWSKI T., *Description of damage and limit conditions for ceramic materials* [in Polish], Lublin University of Technology Press, Lublin, 1999.

*Received October 15, 2016; accepted version November 15, 2016.*

---